Polymer Journal, Vol. 5, No. 1, pp 11—24 (1973)

Thermodynamic Studies of Solid Polyethers. II. Heat Capacity of Poly(oxacyclobutane), $-[-(CH_2)_3O-]_{\overline{n}}$, between 1.4 and 330°K

Shohei YOSHIDA,* Hiroshi SUGA, and Syûzô SEKI

Department of Chemistry, Faculty of Science, Osaka University, Toyonaka, Osaka Japan.

(Received October 7, 1972)

ABSTRACT: Heat capacities of poly(oxacyclobutane), subject to three kinds of thermal history, were measured in the temperature region from liquid helium temperature (1.4°K) to 330°K by using two kinds of adiabatic calorimeters and the effect of thermal treatment upon heat capacity was studied. As a result, it was found that the effect of thermal treatment was evident in the low temperature region (below 15°K) as well as around the glass transition region.

Furthermore, the heat capacity of the completely crystalline state was estimated and analysed, based on Tarasov's model, between 13 and 250°K. Characteristic temperatures θ_1 and θ_3 in Tarasov's model were evaluated to be 605 and 97°K, respectively. Below 13°K, the temperature dependence of the heat capacity was examined for crystalline, semicrystalline, and glassy states.

KEY WORDS Poly(oxacyclobutane) / Heat Capacity / Thermal Treatment Effect / Low Temperature / Glass Transition / Tarasov's Model / Crystallinity Dependence /

In a previous paper,[1] we reported the results of a thermodynamic study of Poly(oxacyclobutane) (abbreviated as POCB). There, we compared the thermodynamic properties of its crystalline state with those of the amorphous one by measuring the heat capacity above 80°K and studied in addition the state of its hydrate by measuring its dissociation pressures.

In the present investigation, heat capacities were measured in a wider temperature region, from liquid helium temperature (1.4°K) to 330°K, by using two kinds of adiabatic calorimeters the thermal treatment effect or crystallinity dependence upon heat capacity was also examined. As was reported[1] POCB is usually a crystalline polymer, but it is possible to attain a completely glassy state by rapid cooling of the melt. In this respect, POCB seems to be a suitable substance for studying the thermal treatment effect.

The thermal treatment effect or crystallinity dependence on heat capacity for solid high polymers has been investigated by several workers above the glass transition region (T_g) but never in the temperature region below T_g. Reese and Tucker[2] have studied the crystallinity dependence for polyethylene. They investigated the relation between heat capacity and crystallinity for three kinds of samples synthesized by different methods. Thus, there remains a possibility that their results may contain not only the effect of the crystallinity, but also the effect of chemical differences such as side groups.

In the present investigation, the crystallinity dependence of the heat capacity was studied by measuring the heat capacities of three samples which were chemically the same but were subjected to different thermal treatments. This dependence was consistently investigated in low temperature regions below T_g as well as in the glass transition region.

Tarasov[3] proposed a model for lattice vibrations in anisotropic crystals such as selenium, graphite, etc., by adapting Debye's model. Wunderlich[4] explained the heat capacity of

* Present Address: *Ashigara Research Laboratory, Fuji Photo Film, Co., Minamiashigara, Kanagawa.*

polyethylene along this line. In the present investigation, we analysed the heat capacities of the completely crystalline state between 13 and 250°K, based on Tarasov's model, in order to investigate the relation between heat capacity and lattice vibrations. Furthermore, below 13°K, the temperature dependence in the heat capacity was examined for the crystalline, semicrystalline, and glassy states.

As was reported,[1] there are three kinds of modification: modification-I, -II, and -III,[5] in the crystalline part of POCB. In the present investigation, for the crystalline part, only modification-III was investigated.

EXPERIMENTAL

Preparation of POCB

The sample was synthesized in the same way as before,[1,6] by using $(C_2H_5)_2OBF_3$ as a catalyst. POCB thus synthesized was further purified by repeated precipatation from methanolic solution with water and dried under vacuum (10^{-5} mmHg) for a week. During this drying procedure, the temperature of the sample was varied to undergo the crystallization and melting process. With this procedure, volatile impurities such as non-reacted monomens were removed as much as possible.

Infrared spectra of the sample which was thus purified were taken for identification. In addition, an X-ray photograph of the sample crystallized from the melt was taken and confirmed to be modification-III.[1,5]

The average molecular weight was obtained by two methods: viscosity measurement and vapor-pressure osmometry. The viscosity was measured in benzene solution at 30°C and the limiting viscosity number was found to be 0.52 dl/g. From this data, the weight-average molecular weight was calculated to be *ca.* 2×10^4, using the data of Fujita, *et al.*[7] Another method yielded the number-average molecular weight, 1.1×10^4.

Measurement of Heat Capacity

Prior to the precise measurement of heat capacity, a preliminary experiment was carried out by using DTA and DSC (DSC-1B) (Perkin-Elmer) apparatuses in order to determine approximate values of the temperatures of glass transition, crystallization, and melting.

Two types of calorimeter were used in the measurement of heat capacity. One of them is an isoperibol calorimeter[8] designed for heat capacity measurement in the temperature region from 1.4 to 20°K. The thermometer used was a germanium-resistance thermometer (Honeywell Series II). The sample container was made of copper, with a capacity of about 100 cm^3. In the temperature region from 11 to 330°K, an adiabatic-type carorimeter[9] was employed. The thermometer used was a platinum-resistance thermometer manufactured by Tinsley Co. This thermometer was calibrated by comparison with a platinum-resistance thermometer calibrated at the U.S. National Bureau of Standards. The sample container was made of gold, with a capacity of about 30 cm^3. Thus, measurement of heat capacity used two different methods in the two temperature regions, *i.e.*, 1.4 to 20°K and 13 to 330°K. The procedures of measurement in these temperature regions are explained below.

In the lower temperature region, the sample weight used was *ca.* 45 g. The sample was put into a sample container and sealed with solder under vacuum. Helium gas, which was usually introduced as the heat exchange medium, was not introduced, in the sample container, because thermal contact between the sample and the container was considered to be good as a result of the thermal treatment described below. In this temperature region, heat capacities were measured for the annealed and rapidly cooled samples. The annealed sample (sample-L1) was prepared by the procedure given below. The temperature of the sample container was first raised up to 325°K, which was higher than the melting temperature found by DSC. Thereafter, the sample container was kept at about 273°K for three days and chilled down to 80°K at a cooling rate slower than 5°K/hr. In the preparation of the rapidly cooled sample (sample-L2), the sample container was first kept at 325°K for 1 hr and quickly chilled down to 80°K at a cooling rate faster than 20°K/min. After these procedures, the apparatus was cooled down to liquid helium temperature. The measurement was performed three times. The heating rate was 0.5 to 3°K/hr. An intermittent heating

technique was employed, with the temperature intervals ranging from 0.1 to 3°K. Time for equilibration was found to be 5 to 15 min. From this fact, the thermal contact between the sample and the container was confirmed to be good.

In the higher temperature region, *i.e.*, 13 to 330°K, the weight of sample used was *ca.* 10 g. The sample was put into the sample container, evacuated, and sealed together with helium gas at 1 atm as the heat exchanger. In this temperature region heat capacity was measured for three samples subjected to different thermal treatments. Two of these, the annealed (sample-H1) and the rapidly cooled one (sample-H2), were subjected to the thermal treatments rather similar to those in the measurement in the liquid helium temperature region. During the rapid cooling, the temperature of the sample was read with a resistance recorder (Leeds & Northrup, Speedmax Type G). The cooling rate was faster than 20°K/min and there was no indication of a crystallization effect in the resistance *vs.* time curve. The third sample (sample-H3) was that which was crystallized around 215°K from the super-cooled liquid during the measurement of the sample-H2. That is, this sample was partially crystallized far below the melting point, but did not undergo an planned annealing procedure. It might be a problem whether this sample was homogeneous or not. As is well known, in the measurement of heat capacity with an adiabatic calorimeter the data obtained corresponds to those for the equilibrium or quasi-equilibrium state. In the present case, the sample-H2 began gradually to crystallize near 215°K during the measurement. From these facts, it was considered that the nuclei of crystal were generated homogeneously in the super-cooled liquid. The measurement of heat capacity was carried out for samples-H1 and -H2 in the temperature region from 13 to 330°K and 13 to 215°K, respectively. As for sample-H3, the heat capacity was measured in two temperature regions, 13 to 60°K and 150 to 230°K, where the heat capacities might show a noticeable dependence on the thermal treatment. The heating rate adopted was 3 to 7°K/hr during the measurement. The temperature steps of the measurement were about 1 to 2°K in the solid and liquid hydrogen temperature regions and 3 to 6°K in the higher temperature region. Time for equilibration was found to be about 5 min in the liquid hydrogen temperature region and 10 to 15 min in the higher temperature region, although it increased in the vicinity of the transition temperature region.

RESULTS AND DISCUSSIONS

Heat Capacity Data

The heat capacity values obtained in the temperature region from 1.4 to 20°K are plotted in Figure 1 and the data are given in Tables I and II. Figures 2 and 3 show the heat capacity values obtained over the temperature region from 13 to 330°K; these data are given in Tables III, IV, and V. The temperature regions in these two works overlapped between 13 to 20°K, where the heat capacity values deviated from each other. These features are shown in Figure 4. The deviations between these dada are larger than the experimental error and may be attributed to a difference in the crystallinity. Though the samples-L1 and -L2 were subjected to thermal treatments similar to those for the samples-H1 and -H2, their crystallinities were considered to be different because of the difference in the amount of the samples used and

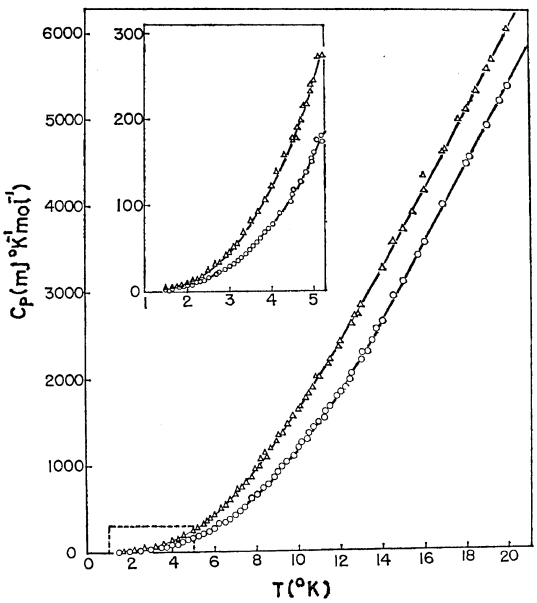

Figure 1. Heat capacity of POCB: ○, sample-L1; △, sample-L2.

Table I. Heat capacity of POCB (sample-L1)

T/K	C_p/JK^{-1} mol^{-1}	T/K	C_p/JK^{-1} mol^{-1}
1st series		6.12	0.2881
4.42	0.1039	6.43	0.3375
4.55	0.1170	6.75	0.3919
4.68	0.1268	7.08	0.4505
4.81	0.1375	7.42	0.5221
5.18	0.1708	8.19	0.6976
5.31	0.1827	8.59	0.7931
5.46	0.1979	9.00	0.9078
5.63	0.2199	9.44	1.029
5.83	0.2469	9.88	1.160
6.22	0.3046	10.30	1.318
6.43	0.3377	10.73	1.425
6.65	0.3623	11.26	1.599
6.87	0.4093	11.89	1.803
7.10	0.4558	12.52	2.036
7.35	0.5027	13.15	2.264
7.60	0.5593	3rd series	
8.10	0.6812	1.47	0.00360
8.35	0.7359	1.64	0.00400
8.62	0.8071	1.80	0.00575
8.90	0.8935	1.92	0.00645
9.20	0.9773	2.03	0.00660
9.50	1.065	2.12	0.01167
9.82	1.167	2.22	0.01010
10.16	1.253	2.34	0.01202
10.52	1.378	2.50	0.01550
11.26	1.640	2.68	0.01986
12.27	1.852	2.84	0.02459
13.03	2.285	3.01	0.02955
13.70	2.565	3.19	0.03574
14.57	2.944	3.37	0.04296
15.68	3.417	3.55	0.05215
16.87	3.999	3.72	0.06035
18.18	4.554	3.90	0.06778
19.62	5.228	4.08	0.08218
2nd series		4.28	0.09119
1.58	0.00176	4.50	0.1148
1.88	0.00592	4.73	0.1294
2.00	0.00714	4.95	0.1507
2.11	0.00795	5.15	0.1699
2.21	0.01138	5.36	0.1920
2.30	0.01115	5.58	0.2146
2.40	0.01272	5.88	0.2531
2.51	0.01617	6.20	0.2986
2.68	0.02055	6.52	0.3534
2.89	0.02569	6.87	0.4253
3.08	0.03226	7.26	0.4882
3.26	0.03819	7.68	0.5779
3.47	0.04580	8.13	0.6809
3.65	0.05652	8.59	0.7912
3.83	0.06818	9.07	0.9321
4.17	0.08056	9.58	1.074
4.52	0.1038	10.00	1.225
4.94	0.1506	10.63	1.390
5.20	0.1737	11.22	1.587
5.51	0.2060	11.85	1.795
5.81	0.2441		

Table II. Heat capacity of POCB (sample-L2)

T/K	C_p/JK^{-1} mol^{-1}	T/K	C_p/JK^{-1} mol^{-1}
1st series		3.52	0.08131
4.58	0.1764	3.68	0.09223
4.68	0.1999	3.83	0.1052
4.81	0.2179	3.98	0.1210
4.95	0.2417	4.12	0.1387
5.09	0.2497	4.29	0.1587
5.22	0.2797	4.50	0.1785
5.36	0.3321	4.78	0.2182
5.50	0.3270	5.29	0.2961
5.65	0.3532	5.54	0.3546
5.80	0.3816	5.78	0.3649
6.39	0.5092	6.01	0.4195
6.58	0.5541	6.22	0.4716
6.76	0.5917	6.44	0.5205
7.12	0.6217	6.67	0.5759
7.31	0.7372	6.95	0.6349
7.53	0.7959	7.16	0.7426
7.75	0.8554	7.47	0.7856
7.97	0.5771	7.79	0.8756
8.21	1.073	8.10	0.9791
8.46	1.081	8.41	1.255
8.71	1.189	8.76	1.400
8.97	1.257	9.09	1.336
9.25	1.359	9.47	1.463
9.51	1.461	9.88	1.615
9.79	1.555	10.33	1.802
10.08	1.661	10.84	2.036
10.39	1.765	11.40	2.182
10.70	1.883	11.97	2.405
11.04	2.034	12.76	2.711
11.47	2.165	14.54	3.564
11.97	2.375	15.40	3.906
12.83	2.721	3rd series	
14.00	3.243	2.23	0.01469
15.06	3.746	2.40	0.02137
15.97	4.408	2.55	0.02583
16.85	4.604	2.75	0.03417
17.67	5.009	2.93	0.04300
18.49	5.330	3.11	0.05265
19.28	5.718	3.33	0.04905
20.00	6.013	3.52	0.08177
2nd series		3.76	0.1014
1.63	0.00551	4.02	0.1282
1.77	0.00854	4.30	0.1561
1.86	0.00970	4.60	0.1917
1.93	0.01051	4.91	0.2336
2.14	0.01435	5.22	0.2788
2.25	0.01475	5.55	0.3378
2.46	0.02283	5.90	0.4027
2.55	0.02601	6.27	0.4815
2.68	0.03073	6.63	0.5692
2.77	0.03250	6.97	0.6527
2.91	0.04215	7.20	0.7088
3.18	0.05523	7.52	0.8983
3.35	0.06830	7.91	1.011

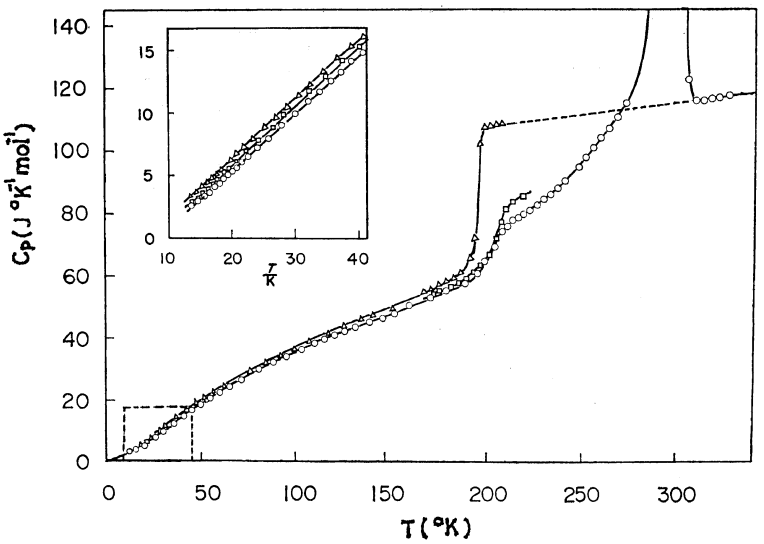

Figure 2. Heat capacity of POCB: ○, sample-H1; △, sample-H2; □, sample-H3.

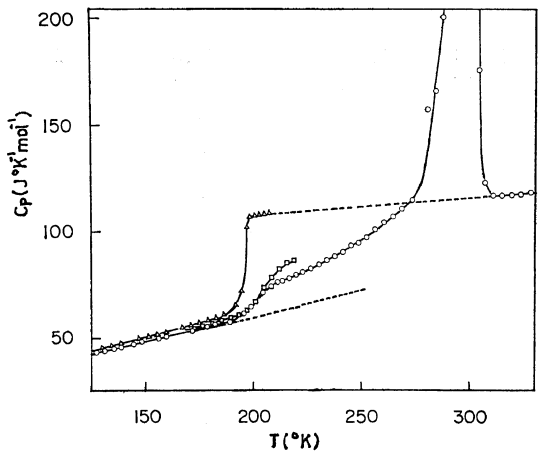

Figure 3. Heat capacity of POCB: ○, sample-H1; △, sample-H2; □, sample-H3.

the difference in the operation of the apparatuses. Details concerning this point will be given below.

Next, we should like to explain briefly the general behavior of the heat capacity. As is shown in Figures 1 and 2, the ratio of the difference between the heat capacities of the annealed and the rapidly cooled samples to the total value is considerable below 20°K. On the other hand, above 20°K, it decreases with rising temperature and reaches 3% at 120°K. This difference remains almost constant up to 150°K and begins to increase gradually up to 185°K. The heat capacity of the sample-H2 shows a steeper increase between 193 and 198°K, where the glass-transition phenomenon takes place. This sample began to crystallize gradually around 215°K and above this temperature shows noticeable crystallization. As shown in Figures 2 and 3, the difference between the extrapolated values of the heat capacities of the melt and the observed heat capacities of the supercooled liquid just above T_g were negligible within the experimental errors. In passing, it may be added that there was no indication of a crystallization effect in the period of preparing sample-H2. Judging from these two facts, sample-H2 was considered to be almost 100-% amorphous.

The sample-H3, crystallized at low temperature and not subjected to planned annealing, had T_g in the range from 195 to 205°K. Above this temperature region, exact measurement was impossible due to as abnormal temperature drift arising from an annealing and/or crystallization effect.

On the other hahd, T_g of the sample-H1 was in the temperature region from 197 to 205°K. Above T_g, the heat capacities of this sample showed a steady rise up to the melting point. The melting region extended from 250 to 300°K. The melting point, T_m, (310°K) in this work was defined as the temperature where the

Table III. Heat capacity of POCB (sample-H1)

T/K	C_p/JK^{-1}mol^{-1}	T/K	C_p/JK^{-1}mol^{-1}
13.60	2.430	120.47	41.40
14.71	2.861	123.98	42.14
15.66	3.380	127.57	43.16
16.53	3.643	131.27	43.88
17.33	4.108	135.05	44.93
18.07	4.475	138.89	45.68
18.77	4.767	144.57	47.16
19.45	5.057	148.41	48.22
20.13	5.382	156.00	49.84
20.83	5.673	159.69	50.80
21.61	6.084	171.54	53.26
22.67	6.559	178.70	55.28
24.12	7.249	185.60	57.08
25.98	8.101	189.02	57.67
27.99	9.068	192.40	57.84
30.08	9.908	195.72	61.72
32.13	10.95	198.96	64.85
33.99	11.71	202.15	69.40
35.70	12.59	204.30	71.76
37.30	13.28	208.10	74.50
38.96	14.15	213.91	77.07
40.67	14.83	216.77	78.37
42.30	15.28	219.60	79.89
43.85	16.14	222.86	81.33
45.05	17.04	226.54	82.96
46.37	17.10	230.27	84.99
48.11	18.18	234.06	86.72
49.85	18.53	237.80	88.59
52.02	19.59	241.50	90.41
54.82	20.65	248.71	94.95
60.04	22.41	252.23	97.77
61.87	22.90	256.14	101.1
63.97	24.00	260.41	104.3
66.33	24.65	264.60	107.2
68.95	25.93	268.69	110.8
71.84	27.35	273.51	115.3
74.78	28.10	280.72	157.8
77.79	29.02	284.36	166.2
80.71	30.11	287.56	200.5
83.55	31.05	290.73	250.3
88.58	32.46	293.58	620.0
95.20	34.61	304.69	176.8
99.03	35.64	307.13	123.4
102.77	36.65	310.78	117.1
106.44	37.53	314.99	117.3
110.04	38.60	319.15	117.5
113.57	39.49	323.74	117.6
117.05	40.41	328.27	118.5

Table IV. Heat capacity of POCB (sample-H2)

T/K	C_p/JK^{-1}mol^{-1}	T/K	C_p/JK^{-1}mol^{-1}
13.61	4.130	80.46	30.78
14.52	4.241	84.42	32.03
15.37	4.325	88.35	33.22
16.18	4.437	92.57	34.71
16.95	4.787	96.27	35.90
17.69	5.097	99.88	36.95
18.40	5.481	103.53	37.76
19.12	5.801	107.81	39.12
19.88	6.221	112.59	40.32
20.79	6.752	117.25	41.78
21.96	7.279	121.24	42.68
23.43	7.986	125.52	43.90
25.23	8.915	130.06	45.06
27.02	9.680	134.50	46.27
28.76	10.50	138.88	47.34
30.60	11.40	147.42	49.55
32.42	12.29	151.60	50.76
34.48	13.38	155.73	51.66
36.74	14.43	159.80	52.71
38.83	15.39	167.26	55.12
40.85	16.17	171.22	55.92
42.92	17.07	175.12	57.30
45.07	18.01	179.01	58.47
47.29	19.08	182.86	59.18
49.48	20.24	186.23	61.06
51.72	20.90	191.90	65.76
54.02	21.56	194.60	72.13
56.58	22.77	196.92	102.4
59.50	23.94	198.97	107.4
62.53	24.96	200.98	107.7
65.61	26.01	202.98	107.9
68.64	26.91	204.98	108.4
72.26	28.06	207.29	108.9
76.44	29.48		

temperature drift became normal. Accordingly, this definition might be looked upon as a calorimetric one, which corresponds with Flory's viewpoint.

Crystallinity and Effect of Thermal Treatment

As was mentioned in the preceding section, there is a distinct difference in heat capacities among the samples subjected to different thermal treatments. The effect of thermal treatment appeared most noticeably in the glass transition and low temperature regions. In order to understand this fact more quantitatively, the thermal treatment effect was considered in terms

of the numerical value of crystallinity.

The crystallinity is generally estimated by various methods such as a density measurement, an X-ray measurement, and others. One of these methods is a calorimetric one. Dole[10] has pointed out the utility of this method. In the present investigation, the crystallinity was evaluated by using the heat capacity values according to Dole's proposal.

The crystallinity of the samples used in the measurement between 13 and 330°K were evaluated in the following way.

By postulating an expected value for the heat capacity of the completely crystalline state, the first approximate value of crystallinity for sample-H1 was estimated at 210°K, under the assumption of a completely amorphous state for the sample-H2 (see last section). Utilizing this first approximate value of crystallinity, the heat capacities of the completely crystalline state were estimated between 13 and 185°K. By extrapolating this curve further up to 210°K, the second approximate value of the crystallinity of the sample-H1 was evaluated. By repeating this procedure, the most plausible value for the crystallinity of sample-H1 was calculated to be 70.1%. Based on this value, the heat capacities of the completely crystalline state were estimated between 13 and 185°K. These heat capacity values are given in Table VI. The data above

Table V. Heat capacity of POCB (sample-H3)

T/K	C_p/JK^{-1}mol^{-1}	T/K	C_p/JK^{-1}mol^{-1}
13.64	2.910	47.25	18.62
14.64	3.256	49.56	19.00
15.53	3.557	52.28	20.35
16.35	3.935	55.50	21.63
17.14	4.346	65.90	25.46
17.89	4.729		
18.65	5.041	172.36	54.60
19.60	5.556	176.85	55.79
20.82	6.130	181.14	56.89
22.40	6.976	185.23	58.07
24.39	7.868	189.26	59.26
26.36	8.791	193.31	61.10
28.23	9.881	197.30	62.80
32.34	11.73	201.19	67.24
34.97	12.95	204.92	73.59
37.55	14.12	208.49	78.75
40.11	15.27	211.97	82.69
42.57	16.34	215.32	85.63
44.92	17.33	218.69	88.64

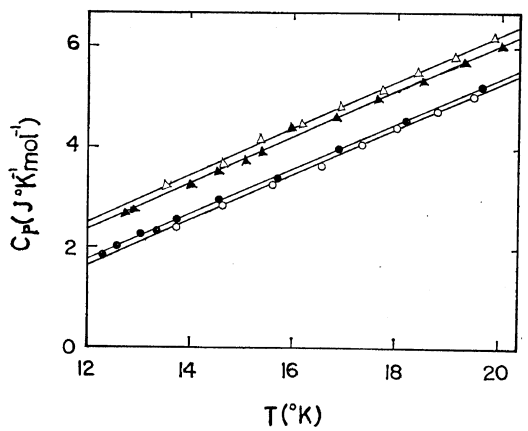

Figure 4. Heat capacity of POCB: ○, sample-H1; △, sample-H2; ●, sample-L1; ▲, sample-L2.

Table VI. Heat capacity of POCB (completely crystalline state)

T/K	C_p/JK^{-1}mol^{-1}	T/K	C_p/JK^{-1}mol^{-1}
13	1.85	80	29.40
14	2.26	85	31.05
15	2.84	90	32.66
16	3.14	95	33.09
17	3.60	100	35.41
18	4.02	105	36.75
19	4.46	110	38.02
20	4.92	115	39.31
22	5.78	120	40.53
25	7.17	125	41.81
27	8.06	130	43.02
30	9.41	135	44.06
33	10.77	140	45.50
35	11.66	145	46.49
38	12.92	150	47.52
40	13.82	155	48.61
43	15.12	160	49.61
45	15.98	165	50.65
48	17.30	170	51.68
50	18.10	175	52.79
55	20.11	180	53.99
60	22.06	190	56.55
65	24.00	200	59.98
70	25.81	230	68.12
75	27.63	250	74.03

190°K in this table are the extrapolated values.

As for sample-H3, the temperature drift in the measurement was abnormal around T_g. This might be due to annealing which took place during the measurement. However, below 180°K (below T_g) the crystallinity of sample-H3 was evaluated consistently to be 41% if we used the relationship between the crystallinity and the heat capacity based on the data for samples-H1 and -H2.

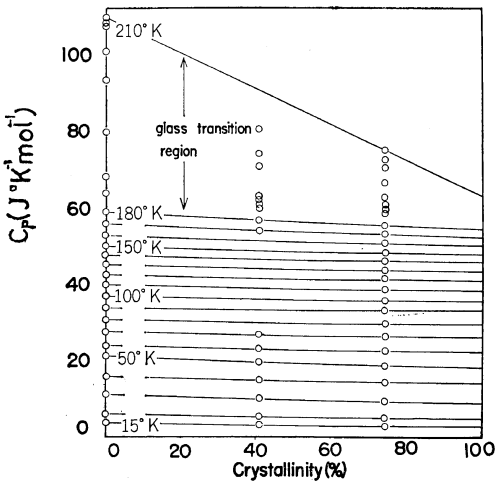

Figure 5. Crystallinity dependence of heat capacity for POCB.

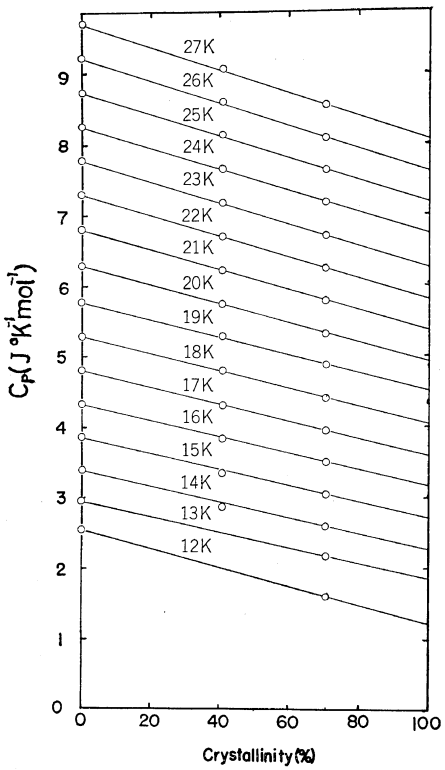

Figure 6. Crystallinity dependence of heat capacity for POCB.

This relationship for the temperature regions of 13—210°K and 12—27°K are shown in Figures 5 and 6 respectively. From this result, the crystallinity dependence of the heat capacity was found to be approximately linear below T_g within deviations of ±2%. The nonlinearity in the glass transition region might be due to intimate interaction between the crystalline and the amorphous parts. This interaction may affect strongly the relaxation phenomenon of the glass transition. Indeed, samples-H1, -H2 and -H3 showed different glass-transition temperatures, as is shown in Figure 3.

We should like to proceed to the same kind of discussion of the heat capacity between 1.5 and 20°K. The heat capacity values measured in this region showed a discrepancy from the data given above in the region from 13 to 20°K (see Figure 4). This may be due to a difference in the crystallinities of the samples used. Therefore, the crystallinities of the samples-L1 and -L2 were evaluated by use of the relation of crystallinity dependence for the results above 13°K. As the result, the crystallinity of the samples-L1 and -L2 was calculated to be 64% and 16% respectively.

By using these two values, the heat capacities of the completely amorphous state (glassy state) and the completely crystalline state were estimated between 1.5 and 20°K. As the crystallinity had an ambiguity of about ±3%, the heat capacity data have an uncertainty of ±13% at 4°K. Figure 7 shows the procedure for estimation of the heat capacity of the completely crystalline as well as the amorphous state in the temperature region from 1.5 to 11°K.

In order to emphasize the crystallinity dependence of the thermal treatment effect, the ratio C_p^s/C_p^c was plotted against log T, where C_p^c is the heat capacity of the completely crystalline state and C_p^s, the sample heat capacity. In Figure 8, this ratio is plotted against log T. The effect is represented more remarkably in this

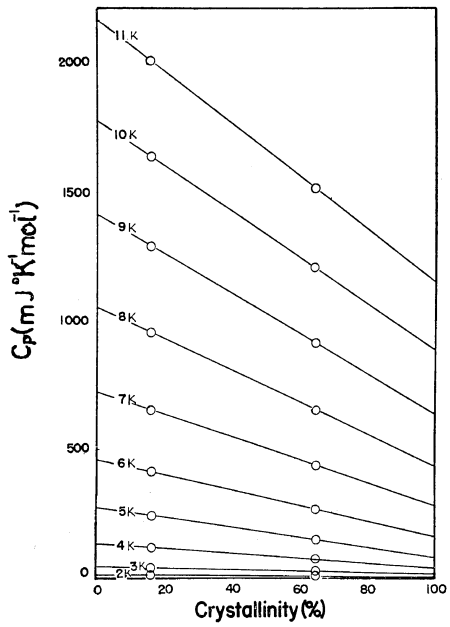

Figure 7. Estimation of heat capacity of completely crystalline and amorphous states for POCB.

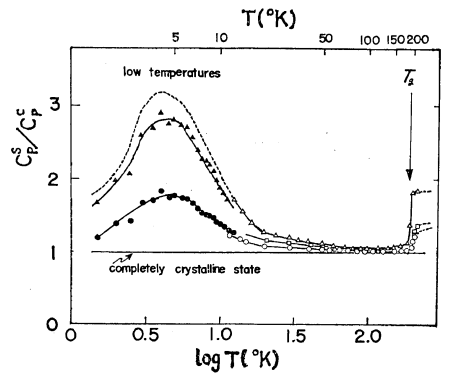

Figure 8. Thermal treatment effect on heat capacity for POCB: C_p^s/C_p of sample, C_p^c/C_p of completely crystalline state: ●, sample-L1; ▲, sample-L2; ○, sample-H1; △, sample-H2; □, sample-H3; ——, completely crystalline state; - - -, completely amorphous state.

figure. Although the crystallinity dependence is found in all temperature regions, it is particularly noticeable both in the low temperature region (below 10°K) and in the glass transition region.

The origins of the crystallinity dependence in these two temperature regions may be, however, different from each other. One origin will be the relaxation phenomenon of the molecular motion in the amorphous state and the other will be the difference in vibration spectra between the crystalline and amorphous states.

Reese, *et al.*,[2] have investigated the crystallinity dependence of the heat capacity for polyethylene. They have measured the heat capacity of different samples, for which the crystallinities were controlled in the course of synthesis of the samples. There is the possibility that their results may contain not only the effect of the crystallinity but also the effect of chemical impurity such as side groups.

On the other hand, in the present investigation, the crystallinity was controlled only by thermal treatment. In this sense, the present investigation will be the first time that the thermal treatment effect was systematically investigated from the lowest temperature to the glass transition temperature regions.

Heat Capacity at Constant Volume

For the same of theoretical discussion, the heat capacity at constant volume is more convenient. Since we have no data of isothermal conpressibility and thermal expansion coefficient, we used the equation of Nernst and Lindemann,[11] as given below:

$$C_p - C_v = C_v^2 T \text{ const.}$$

This equation can be rewritten as follows:

$$C_p - C_v = C_p^2 (T/T_m) A_0$$

where A_0 is 0.0214 cal^{-1}°K mol, a universal constant. Wunderlich[12] estimated this constant, A_0, to be 0.0203 cal^{-1}°K mol for polyethylene by using thermodynamic data such as compressibility, expansion coefficient, and specific volume. According to his result, this relationship can be considered to be almost valid for polymer substances.

In applying this relationship to POCB, another problem exists in the ambiguity of the definition of mole.

In the present investigation, we approximated the value A_0 which was obtained by dividing the value, A_0, for polyethylene by the number of groups in the repeating unit in the present substances. That is, the value of 0.00122 J^{-1}°K mol was used as the constant, A_0, for POCB. The

difference between C_v and C_p starts to exceed the experimental error around 40°K. Above this temperature, this difference became gradually larger and amounted to about 5% of C_p at 200K.

Normal Vibration of POCB Molecule

Infrared and Raman spectra of POCB have been measured by Tadokoro, *et al.*[13] They analysed the normal vibration of the single chain of POCB. According to their results, the POCB molecule belongs to D_2 and there are four kinds of symmetry species: A, B_1, B_2, and B_3 in the point group D_2. The data for the normal vibration belonging to A is not reported. In order to estimate roughly the dispersion of the normal vibrations, all the frequency values were plotted for two extreme cases of δ (phase difference)$=0$ and $\delta=\pi$. B_1 is optically active at $\delta=0$ and B_2 as well as B_3 are optically active at $\delta=\pi$. Figure 9 shows these results.

The 30 normal vibrational modes of POCB per chemical repeating unit are roughly classified into the CH_2 stretching, bending, wagging, twisting, and rocking modes and the skeletal stretching, bending, and torsional modes. These vibrational modes would have distributions of frequencies but the progression of the frequency within each distribution is completely unknown.

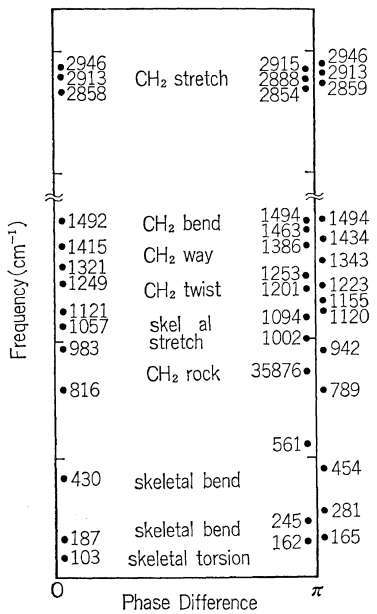

Figure 9. Normal vibrations of POCB.

Table VII. Vibrations of POCB

Vibrational mode	Aevrage frequency, ν/cm^{-1}	Characteristic temperature, θ_E/K	Number of modes
CH_2 asym stretch.	2924	4208	3
CH_2 sym stretch.	2867	4126	3
CH_2 bend.	1483	2134	3
CH_2 wag.	1379	1984	3
CH_2 twist.	1231	1771	3
Skeletal stretch.	1091	1570	4
CH_2 rock	881	1268	3
Skeletal bend.	561	807	1
Other modes	Tarasov's spectra		7
			30

The CH_2 stretching has a very high frequency and gives rise to a narrow distribution. The CH_2 bending, wagging, twisting, and rocking modes are found approximately from 1494 to 1463 cm^{-1}, from 1434 to 1321 cm^{-1}, from 1253 to 1201 cm^{-1} and from 938 to 789 cm^{-1}, respectively. The skeletal stretching mode appears in the neighborhood of 1155 to 1002 cm^{-1}. The skeletal bending and torsional modes, which have lower frequencies than those of the vibrational modes mentioned just above, would show extremely broadly extended distributions of frequencies.

The average frequency of each of these modes and the corresponding characteristic temperature, θ_E, are given in Table VII. The maximum frequency of each skeletal bending modes and its characteristic temperature are also given in this table since these values are necessary for the analysis of heat capacity data.

Calculation of the Heat Capacity above 13°K

In this investigation, Tarasov's model will be utilized in order to analyse the heat capacity data of the completely crystalline state of polyoxacyclobutane. For convenience in the discussions given below, the outline of Tarasov's model is briefly explained.

For linear lattices, Tarasov postulated that of the $3N$ possible normal modes of the solid, $3N_3$ were distributed according to the normal three-dimensional distribution and $3N_1$ according to a linear continuum. Thus the frequency distribution is

$$g(\nu)=9N_3\nu_3^{-3}\nu^2 d\nu \qquad (0<\nu<\nu_3)$$
$$=3N_1(\nu_1-\nu_3)^{-1}d\nu \qquad (\nu_3<\nu<\nu_1),$$
$$N=N_3+N_1$$

where $g(\nu)$ is the frequency distribution function, ν_3 is the frequency where the three-dimensional continuum goes into the linear continuum and ν_1 is some cut-off frequency. With the further restriction that $N_3=N(\nu_3/\nu_1)$, one obtains for the heat capacity,

$$\frac{C_{1,3}}{R}=D_1(\theta_1/T)-\frac{\theta_3}{\theta_1}[D_1(\theta_3/T)-D_3(\theta_3/T)]$$

where $\theta_1=h\nu_1/k$, $\theta_3=h\nu_3/k$ and $D_1(\theta_1/T)$, $D_3(\theta_3/T)$ are the one-dimensional Debye function and the three-dimensional Debye function respectively. The heat capacity for the limiting case of $\theta_3/\theta_1=0$ and $\theta_3/\theta_1=1$ corresponds to the one-dimensional Debye heat capacity and the three-dimensional one respectively.

Calculation was performed for the heat capacity of the completely crystalline state only between 13 and 250°K by using Tarasov's[3] model. This was due to the fact that the heat capacity data of the completely crystalline state below 13°K might have a larger ambiguity in the estimation of the crystallinity. In such a case, the data above T_g would correspond to the extrapolated values with less reliability.

In the calculation of the heat capacity, the CH_2 group was treated as a solid unit. That is, the heat capacity contributed by the CH_2 groups, which have 18 vibrational modes per repeating unit, was calculated by using Einstein functions with the characteristic temperatures shown in Table VII and they were subtracted from the experimental heat capacity at constant volume. Though these vibrational modes have a distribution of frequencies, it was narrow enough that their contributions could be evaluated by this procedure without any significant loss of accuracy for the temperature region of interest.

The remainder of the heat capacity consists of the contributions from the skeletal vibrations which are principally composed of 4 stretching, 4 bending, and 4 torsional vibrational modes per chemical repeating unit. The first attempt was to approximate the contributions of these 12 skeletal vibrational modes by a Tarasov-type treatment. This was, however, unsuccessful in reproducing well the experimental heat capacities. The same circumstance had also happened in the analysis of heat capacity for polyethylene by Wunderlich.[4] It may be due to the fact that the skeletal stretching modes have very high frequencies compared with the other skeletal vibrational modes as seen in Figure 9.

For this reason, the following second trial was made. The contributions of the 4 skeletal stretching modes among the 12 skeletal modes as well as the contribution of the vibrational modes of the CH_2 groups were subtracted from the experimental heat capacity by using the Einstein function. Then, the remainder, which was chiefly composed of the 8 skeletal vibrational modes per chemical repeating unit was approximated by the Tarasov-type treatment. This approximation was able to explain the experimental heat capacity for the completely crystalline state between 13 and 250°K with a fair amount of success. The characteristic temperatures thus obtained were $\theta_3=97\pm1$°K and $\theta_1=605\pm5$°K for the three-dimensional and one-dimensional parts respectively. Based on this result, the heat capacity of POCB is reproduced by the following relation:

$$C_v=8RC_{1,3}(\theta_1,\theta_3)+4RE(\theta_E{}^s)+R\sum^{18}E(\theta_E),$$
(per mol of repeating unit)

where $C_{1,3}$ is Tarasov's heat capacity function with $\theta_1=605$°K and $\theta_3=97$°K and E the Einstein function with $\theta_E{}^s$ and θ_E for the characteristic temperatures of the skeletal stretching and CH_2 group vibrations respectively. The heat capacities in the extremely low temperature region were expressed by the following equation:

$$C_v=0.911T^3 \text{ mJ°K}^{-1}$$
(per chemical repeating unit)

and θ_D was evaluated to be 178°K by the relation, $\theta_D{}^3=\theta_1\theta_3{}^2$.

The calculated heat capacities are listed in Table VIII together with the experimental heat capacities and deviations from them. Figure 10 represents these values together with the heat capacities approximated by the Tarasov-type treatment and by the Einstein functions. The selected temperatures for tabulation above 200°K are only 230 and 250°K, since the heat capacities

Table VIII. Experimental and calculated heat capacities of POCB

T/K	C_v/R per mole of repeating unit		
	Experimental	Calculated	Deviation, %
13	0.221	0.218	−1.3
14	0.272	0.262	−3.6
15	0.341	0.310	−9.0
16	0.378	0.358	−5.2
17	0.433	0.410	−5.3
18	0.483	0.463	−4.1
19	0.536	0.510	−4.9
20	0.592	0.571	−3.5
25	0.862	0.841	−2.4
30	1.130	1.106	−2.6
35	1.402	1.362	−2.8
40	1.661	1.610	−3.0
50	2.169	2.168	0
60	2.639	2.640	0
70	3.081	3.080	0
80	3.503	3.504	0
90	3.884	3.881	0
100	4.201	4.202	0
110	4.496	4.508	+0.2
120	4.778	4.826	+1.0
130	5.056	5.110	+0.9
140	5.334	5.389	+1.1
150	5.553	5.591	+0.7
160	5.775	5.874	+1.7
170	5.992	6.105	+1.8
180	6.232	6.333	+1.6
190	6.507	6.550	+0.7
200	6.723	6.757	+0.4
230	7.365	7.437	+0.9
250	7.815	7.911	+1.2

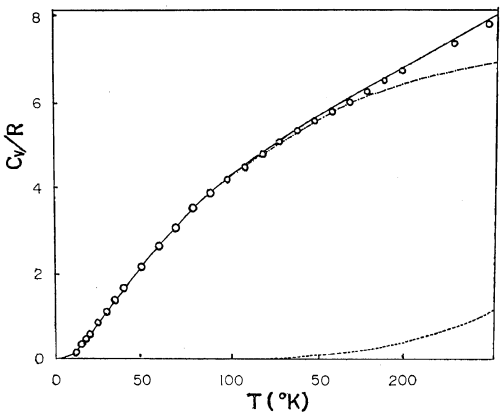

Figure 10. Heat capacity of POCB: ○, exptl; ——, calcd. (total); ·····, Tarasov approximation; – – –, by skeletal strectch. and CH_2 group vibrations.

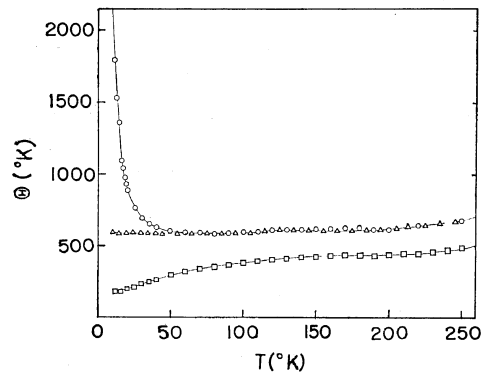

Figure 11. Characteristic temperatures of POCB: (△, θ_1; ○, by one-dimensional Debye function; □, by three-dimensional Debye function.

above the glass transition region are extrapolated values.

The variation of θ_1 with temperature was calculated and is shown in Figure 11 together with the characteristic temperatures based on the one-dimensional and three-dimensional Debye functions. It was found that θ_1 is almost constant between 13 and 250°K. This fact also confirmed that the heat capacity of the completely crystalline state can be reproduced by the summation of Tarasov's equation and Einstein functions. The characteristic temperature of the three-dimensional Debye function changes from about 185 to 485°K, while that of the one-dimensional Debye function is almost constant above 60°K. Thus, the three-dimensional Debye function may not be able to reproduce the heat capacity of POCB, but the one-dimensional Debye function may be able to express approximately the data above 60°K. Further, θ_3/θ_1, is evaluated to be 0.160 by using $\theta_1=605$°K and $\theta_3=97$°K. It is noteworthy that this ratio is very small. These facts imply that the lattice of the crystalline POCB is strongly anisotropic.

As the third trial, it was checked whether the above trial is a unique solution by the Tarasov-type approximation or not. The contribution of one skeletal bending, 4 skeletal stretching, and the CH_2 group vibrational modes were subtracted from the experimental heat capacity by

using Einstein functions. In this procedure, the maximum characteristic temperature of the skeletal bending modes (see Table VII) was used in the calculation of the Einstein function. In this case, the remainder was the contribution of 7 modes of the skeleton per chemical repeating unit. This could be approximated by the Tarasov-type treatment, leading to $\theta_1=500°K$ and $\theta_3=100°K$ for the one-dimensional and three-dimensional parts respectively. In this third trial, the contribution of the 7 skeletal vibrational modes (omitting the one skeletal bending mode) was also approximated by the Tarasov-type treatment.

At the present stage, however, it may be said that the second case seems to be superior to the third one.

In passing, it should be recalled that the condition, $N_3/N=\theta_3/\theta_1$, where N and N_3 are number of total modes and of modes in three dimensional part, was always assumed when we applied Tarasov's mode.

Heat Capacity below 13°K

In Figure 12, C_p/T^3 is plotted against temperature for two samples and for the estimated

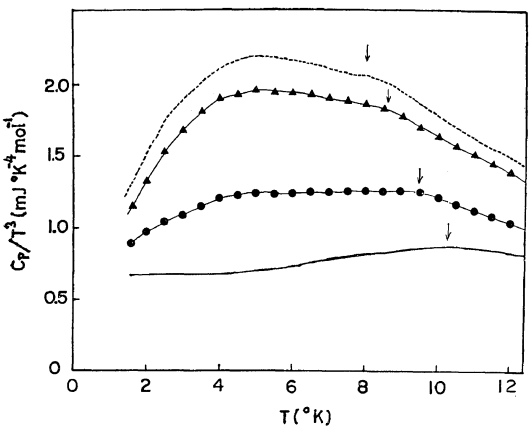

Figure 12. C_p/T^3 *vs.* temperature: ●, sample-L1; ▲, sample-L2; ——, completely crystalline state; – – –, completely amorphous state.

completely crystalline and amorphous states. The values of C_p/T^3 for these two extreme states will include ambiguities since their crystallinities not estimated correctly. For example, the estimated errors of 2% for the crystallinity will produce an uncertaintly of about ±10% for the extrapolations to the completely crystalline and amorphous states around 5°K.

Even though we have this kind of ambiguity in the data, we should like below to draw some interesting and semiquantitative conclusions.

The three curves in Figure 12 for the annealed and rapidly cooled samples, and for the completely amorphous state show a distinct hump with its maximum around 4 to 6°K. This hump seems to arise from the amorphous part since the size of this hump become larger with decreasing crystallinity. This hump may be evidence of an excess heat capacity similar to that[14] found for several glassy solids such as vitreous silica,[15] vitreous germania,[16] and glycerol.[17]

A more detailed inspection of these curves will reveal that they show subhumps, which have maxima displaced to higher temperatures with increasing crystallinity. Possibly affected by this phenomena, even in the completely crystalline state the hump appears to some extent around 10°K.

For the explanation of this phenomenon some origins such as an effect of the side and/or end groups[18] and the uncertainity of assuming a linear relationship between the crystallinity and heat capacity might be considered. It will be, however, difficult to ascertain the true origin at the present stage of investigation. Finally we may add here that the heat capacities of the completely crystalline state show a cubic temperature dependence at least below 5°K.

Acknowledgment. The authors wish to thank Professor H. Tadokoro, Assistant Professor Y. Chatani, and Dr. M. Kobayashi of Osaka University for the detailed information about the structural and spectroscopic data for POCB. Thanks are also due to Professor H. Fujita of Osaka University and Dr. K. Nakao of Industrial Research Institute, Osaka Prefecture, for allowing the authors to use the apparatus for molecular weight measurement and the gel-permeation chromatography apparatus, respectively.

REFERENCES

1. S. Yoshida, M. Sakiyam, and S. Seki, *Polymer J.*, **1**, 573 (1970).
2. W. Reese and O. Tucker, *J. Chem. Phys.*, **46**, 1388 (1967).

3. V. V. Tarasov, "New Problems in the Physics of Glass," Israel Program for Scientific Translations, Jerusalem, 1963.
4. B. Wunderlich, *J. Chem. Phys.*, **37**, 1207 (1962).
5. H. Tadokoro, Y. Takahashi, Y. Chatani, and H. Kakida, *Makromol. Chem.*, **109**, 96 (1967).
6. J. B. Rose, *J. Chem. Soc.*, 526 (1956).
7. K. Yamamoto, A. Teramoto, and H. Fujita, *Polymer*, **7**, 267 (1966).
8. M. Sorai, H. Suga, and S. Seki, *Bull. Chem. Soc. Jap.*, **41**, 312 (1968).
9. T. Matsuo, H. Suga, and S. Seki, *J. Phys. Soc. Jap.*, **30**, 785 (1971).
10. M. Dole, *J. Polymer Sci., Part C*, **18**, 57 (1967).
11. W. Nernst and F. A. Lindemann, *Z. Electrochem.*, **17**, 817 (1911).
12. B. Wunderlich, *J. Chem. Phys.*, **37**, 1203 (1962).
13. D. Makino, M. Kobayashi, and H. Tadokoro, *ibid.*, **51**, 3901 (1969).
14. H. B. Rosenstock, *J. Phys. Chem. Solids*, **23**, 659 (1962).
15. P. Flubacher, A. J. Leadbetter, J. A. Morrison, and B. P. Stoicheff, *ibid.*, **12**, 53 (1959).
16. A. A. Antoniou and J. A. Morrison, *J. Appl. Phys.*, **36**, 1873 (1965).
17. R. S. Craig, C. W. Massena, and R. M. Mallya, *ibid.*, **36**, 108 (1965).
18. G. L. Salinger, C. L. Choy, and R. G. Hunt, *J. Chem. Phys.*, **52**, 3629 (1970).